

## Enhancement of $\alpha$ PNA Binding Affinity and Specificity through Hydrophobic Interactions

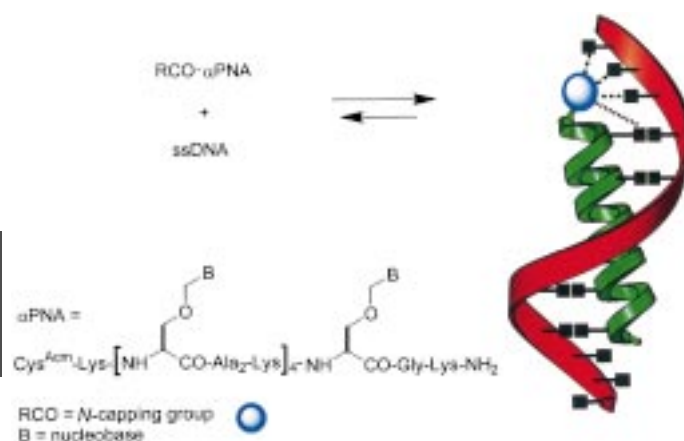
Philip Garner,\* Yumei Huang, and Subhakar Dey<sup>[a]</sup>

### KEYWORDS:

DNA recognition · hydrophobic effect · peptide nucleic acids · stacking interactions · supramolecular chemistry

We recently disclosed that  $\alpha$ -helical peptide nucleic acids ( $\alpha$ PNAs), hybrid molecules that combine structural properties of peptides with the codified molecular recognition elements of nucleic acids, bind to complementary tracks of single-stranded DNA (ssDNA) with high affinity and sequence specificity.<sup>[1]</sup> Under equivalent hybridization conditions,  $\alpha$ PNA·DNA complexes exhibit considerably higher melting temperatures than the corresponding DNA duplexes. An interesting facet of  $\alpha$ PNA·DNA complexation was the preferred directionality of binding, with the “parallel” (N/5′) orientation being favored both thermodynamically and kinetically over the “antiparallel” (N/3′) orientation. This is analogous to the well-known antiparallel (5′/3′) strand orientation which is generally observed in nucleic acid duplexes. Evidence that the parallel complex Ac-CTCCT·d(A<sub>3</sub>-GAGGAA<sub>3</sub>) and its antiparallel counterpart Ac-CTCCT·d(A<sub>3</sub>AGGAGA<sub>3</sub>) (noncomplementary “dangling” bases are italicized) possessed different secondary structures could be gleaned from their circular dichroism (CD) profiles, especially in the 230–290-nm region where the interaction of asymmetrically disposed nucleobases is expected to dominate the CD spectrum.<sup>[2]</sup> The spectrum of the complex formed from an  $\alpha$ PNA with a symmetrical base sequence (Ac-CCTCC), capable of forming either a parallel or antiparallel complex, was consistent with the former orientation.

To gain a better understanding of (and control over) this remarkable platform for nucleic acid recognition, we set out to examine the binding properties of a series of  $\alpha$ PNAs that incorporated a variety of arenyl ( $\pi$ -stacking and hydrophobic effects) as well as aliphatic (hydrophobic effect only) *N*-caps (Scheme 1). (Experimental details for the synthesis, purification, and characterization of *N*-capped  $\alpha$ PNAs, purification protocols for DNAs, thermal denaturation profiles, and CD spectra for  $\alpha$ PNA·DNA complexes can be found in the Supporting Information.) Our design reasoning was based on the assumption that tighter binding would result if “end-fraying” were minimized by incorporating stabilizing interactions at one or both



**Scheme 1.** Proposed model for binding of hydrophobic  $\alpha$ -helical peptide nucleic acids ( $\alpha$ PNAs; shown in green) to single-stranded DNA (ssDNA; shown in red).

ends of the  $\alpha$ PNA chain. This could be important since our  $\alpha$ PNA modules rely on only five base-pair interactions and end-fraying could adversely affect up to 50% (in CTTC) of the interstrand Watson–Crick hydrogen bonds. The enhancement of duplex stability through such  $\pi$ – $\pi$  interactions had been demonstrated with unpaired “dangling” nucleobases at the 5′ ends of RNA,<sup>[3]</sup> and analogous effects were observed when nucleobases as well as their unnatural aromatic counterparts were incorporated at the 5′ ends of DNA.<sup>[4, 5]</sup> A stabilizing effect on oligonucleotide duplexes has also been noted when they were 5′-capped with aliphatic steroids.<sup>[6–8]</sup> We now report that *N*-capped  $\alpha$ PNAs lead to both enhanced affinity as well as orientational specificity with complementary ssDNA targets. Unexpectedly, the observed *N*-cap effects in the preferred parallel series were found to be more strongly correlated to *N*-cap hydrophobicity rather than  $\pi$ -stacking potential.

The *N*-capped  $\alpha$ PNAs were synthesized following our usual solid-phase peptide synthesis (SPPS) protocol, but substituting the appropriate carboxylic acid in the *N*-capping step.<sup>[9]</sup> The *N*-caps investigated consisted of a series of commercially available arenyl-substituted and aliphatic carboxylic acids (Scheme 1). Both sets of *N*-caps included a flexible methylene linker to allow for the anticipated cap–base interaction without significantly disrupting the complex structure. Thermal UV denaturation (given in form of the melting temperature  $T_m$ ) data for the *N*-cap-CTCCT·d(A<sub>3</sub>GAGGAA<sub>3</sub>) (N/5′ or parallel orientation) and *N*-cap-CTCCT·d(A<sub>3</sub>AGGAGA<sub>3</sub>) (N/3′ or antiparallel orientation) complexes are collected in Table 1.<sup>[10, 11]</sup> A number of interesting trends emerge from these data. First, all of the *N*-cap modifications resulted in higher  $T_m$  values for the parallel  $\alpha$ PNA·DNA complexes relative to the “parent” *N*-acetylated compounds. However, contrary to our expectations, the most striking enhancement occurred in the parallel aliphatic *N*-cap series, with the 4-(cyclohexyl)butyryl-*N*-cap resulting in the highest  $T_m$  value (47.9 °C). This represented an increase of 11 °C compared to the parent *N*-acetylated  $\alpha$ PNA. We also prepared a cholic-acid-capped  $\alpha$ PNA to make a comparison with the nucleic acid literature data<sup>[8]</sup> and found that parallel cholyl-CTCCT·d(A<sub>3</sub>GAGGAA<sub>3</sub>) exhibited a  $T_m$  of 45.6 °C. Aliphatic *N*-caps would

[a] Prof. P. Garner, Y. Huang, S. Dey  
Department of Chemistry  
Case Western Reserve University  
Cleveland, OH 44106-7078 (USA)  
Fax: (+1) 216-368-3006  
E-mail: ppg@po.cwru.edu

Supporting information for this article is available on the WWW under <http://www.chembiochem.com> or from the author.

**Table 1.** UV melting data for parallel and antiparallel *N*-capped  $\alpha$ PNA·DNA complexes.

Cap-CTCCT cap =	d(A <sub>3</sub> -GAGGA-A <sub>3</sub> ) <i>T<sub>m</sub></i> [°C] (parallel)	d(A <sub>3</sub> -AGGAG-A <sub>3</sub> ) <i>T<sub>m</sub></i> [°C] (antiparallel) <sup>[a]</sup>
CH <sub>3</sub> CO	37.0	32.0
CH <sub>3</sub> CH <sub>2</sub> CH <sub>2</sub> CO	40.0	30.2
CH <sub>3</sub> CH <sub>2</sub> CH <sub>2</sub> CH <sub>2</sub> CH <sub>2</sub> CO	41.0	33.4
C <sub>3</sub> H <sub>9</sub> CH <sub>2</sub> CH <sub>2</sub> CO	43.7	33.8
C <sub>6</sub> H <sub>11</sub> CH <sub>2</sub> CH <sub>2</sub> CH <sub>2</sub> CO	47.9	33.4
cholyl	45.6	34.6
C <sub>6</sub> H <sub>5</sub> (CH <sub>2</sub> ) <sub>3</sub> CO	41.8	33.6
<i>p</i> -MeOC <sub>6</sub> H <sub>4</sub> (CH <sub>2</sub> ) <sub>3</sub> CO	41.3	34.2
<i>p</i> -NO <sub>2</sub> C <sub>6</sub> H <sub>4</sub> (CH <sub>2</sub> ) <sub>3</sub> CO	41.6	34.4
2-naphthyl-(CH <sub>2</sub> ) <sub>3</sub> CO	42.7	36.3
1-pyrenyl-(CH <sub>2</sub> ) <sub>3</sub> CO	42.6	39.0

[a] No cooperative transition was observed during the cooling cycle.

not be expected to have a greater effect than arenyl *N*-caps if  $\pi$  stacking were responsible for the additional stabilization of these  $\alpha$ PNA·DNA complexes. The relative insensitivity of the melting temperatures of 4-(aryl)butyryl-*N*-capped compounds to substitutions with electron-donating and electron-withdrawing groups is consistent with this interpretation.<sup>[12]</sup>

Analogous *T<sub>m</sub>* enhancements were observed (Table 2) with the symmetrical sequences *N*-4-(cyclohexyl)butyryl-CCTCC·d(A<sub>3</sub>GGAGGA<sub>3</sub>) (60.8 °C) and *N*-4-(cyclohexyl)butyryl-CCCC·d(TA<sub>3</sub>GGGGGA<sub>3</sub>T) (64.9 °C), thus excluding the possibility that these trends were related solely to the base sequence. The

**Table 2.** UV melting data for symmetrical *N*-4-(cyclohexyl)butyryl- $\alpha$ PNA·DNA complexes.

$\alpha$ PNA·DNA complex	<i>T<sub>m</sub></i> [°C]
C <sub>6</sub> H <sub>11</sub> (CH <sub>2</sub> ) <sub>3</sub> CO-CCTCC 5'-d(A <sub>3</sub> -GGAGG-A <sub>3</sub> )-3'	60
C <sub>6</sub> H <sub>11</sub> (CH <sub>2</sub> ) <sub>3</sub> CO-CCCC 5'-d(TA <sub>3</sub> -GGGGG-A <sub>3</sub> T)-3'	65
C <sub>6</sub> H <sub>11</sub> (CH <sub>2</sub> ) <sub>3</sub> CO-CCTCC 5'-d(TA <sub>3</sub> -GGGGG-A <sub>3</sub> T)-3'	50

incorporation of a single base-pair mismatch (*N*-4-(cyclohexyl)butyryl-CCTCC·d(TA<sub>3</sub>GGGGGA<sub>3</sub>T)) lowered the *T<sub>m</sub>* value by 15 °C, which is consistent with our previous observations in the *N*-acetyl series and indicates that the *N*-cap effect is decoupled from base pairing. This reduction in melting temperature presumably arises from residual hydration of the mismatched nucleobases and provides additional support for our proposed Watson–Crick binding model.

In keeping with our earlier studies, the antiparallel *N*-capped  $\alpha$ PNA·DNA complexes exhibited lower *T<sub>m</sub>* values than their parallel counterparts. However, contrary to our results in the parallel series, the highest antiparallel *T<sub>m</sub>* values were obtained with the 4-(2-naphthyl)butyryl and 4-(1-pyrenyl)butyryl *N*-caps (36.3 and 39.0 °C, respectively). In no case was cooperative binding observed during the cooling cycle of these antiparallel melting experiments, indicating relatively slow annealing kinetics. Except for the complexes that incorporate the pyrene

chromophore, the CD spectra of the parallel *N*-capped  $\alpha$ PNA·DNA complexes are nearly superimposable on the CD spectra of the corresponding *N*-acetyl-substituted complexes (see Figure 1 and Supporting Information), suggesting that the *N*-caps are not changing the overall structure of the parallel  $\alpha$ PNA·DNA complexes. Significantly, the *N*-4-(cyclohexyl)butyryl *N*-cap led to enhanced orientational specificity, with  $\Delta T<sub>m</sub>$  (parallel *T<sub>m</sub>* – antiparallel *T<sub>m</sub>*) increasing from 5 to 15 °C.

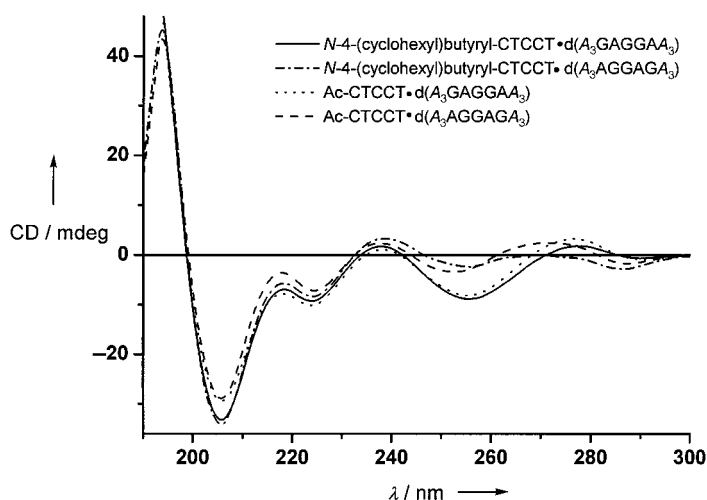


**Figure 1.** Comparative CD spectra of parallel and antiparallel  $\alpha$ PNA·DNA complexes. Samples were made by combining 5  $\mu$ M solutions of each component in HPLC-grade water in a stoppered optical quartz cell (1 cm path length); the spectra were recorded at 5 °C. Nitrogen gas was purged through the sample compartment. Each data point is the average of eight (baseline-corrected) points.

A plot of *T<sub>m</sub>* versus calculated octanol/H<sub>2</sub>O partition coefficients (log *P* values) for each *N*-cap (Figure 2) clearly shows that the melting temperatures of  $\alpha$ PNA·DNA complexes is proportional to *N*-cap hydrophobicity.<sup>[13]</sup> We hypothesize that the strong dependence of *T<sub>m</sub>* on log *P* in the parallel aliphatic *N*-cap series is due to a combination of “classical” (entropically driven) desolvation and “nonclassical” (enthalpically driven) packing hydrophobic effects.<sup>[14]</sup> For the antiparallel complexes, which exhibit uniformly lower *T<sub>m</sub>* values than their parallel counterparts, a weaker dependence is found for the arenyl *N*-caps. This suggests the existence of compensating  $\pi$ -stacking effects superimposed on the hydrophobic effects and is probably related to different overall structures (see CD data, Table 1), but this is still conjecture that will have to await the completion of  $\alpha$ PNA·DNA structural studies. On the other hand, melting temperature is essentially independent of *N*-cap hydrophobicity in both the parallel/aromatic and antiparallel/aliphatic series.

By demonstrating that strategically placed aliphatic groups can be used to modulate the affinity and orientational specificity of  $\alpha$ PNA complexation to DNA, we have expanded the repertoire of binding interactions available to these novel nucleic acid surrogates. These studies provide a direct comparison between aliphatic and aromatic end caps showing that—at least for  $\alpha$ PNAs—the former can have a stronger effect on hybridization than the latter.

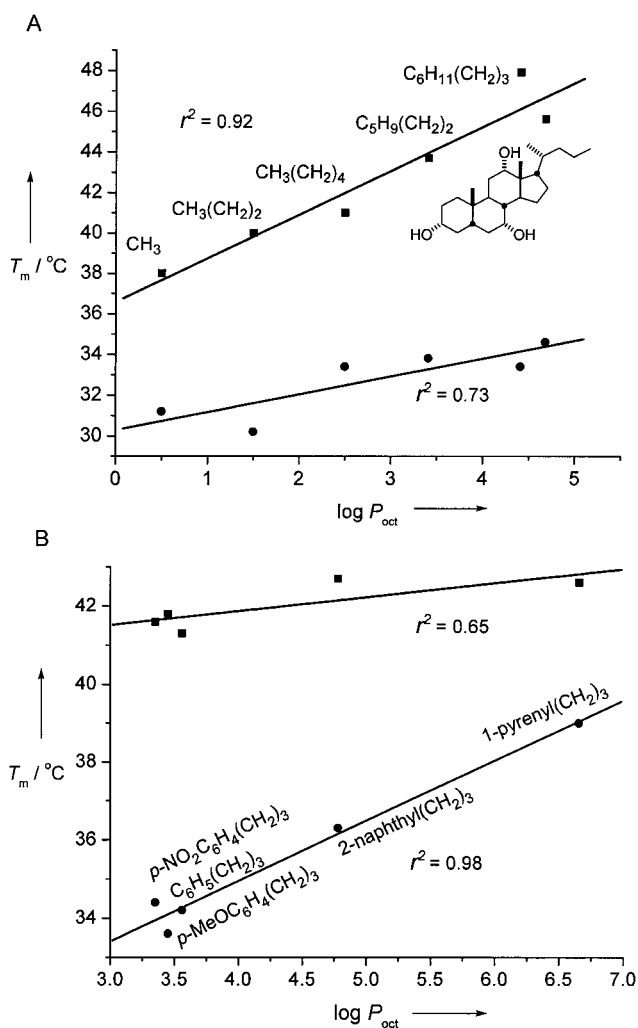


**Figure 2.** Plots of  $T_m$  versus calculated  $\log P$  values for parallel N-capped CTCCT· $d(\text{A}_3\text{GAGGAA}_3)$  (upper data points, ■) and antiparallel N-capped CTCCT· $d(\text{A}_3\text{AGGAGA}_3)$  (lower data points, ●). A: Aliphatic N-caps. B: Arenyl N-caps. The correlation coefficient  $r^2$  (Pearson's correlation) is shown for each data set (see Supporting Information for details).

This work was supported by a grant from the National Institutes of Health (GM54796).

- [1] P. Garner, S. Dey, Y. Huang, *J. Am. Chem. Soc.* **2000**, *122*, 2405–2406.  
 [2] W. C. Johnson, Jr. in *Circular Dichroism and the Conformational Analysis of Biomolecules* (Ed.: G. D. Fasman), Plenum, New York, **1996**.  
 [3] M. Petersheim, D. H. Turner, *Biochemistry* **1983**, *22*, 256–263.  
 [4] M. Senior, R. A. Jones, K. J. Breslauer, *Biochemistry* **1988**, *27*, 3879–3885.

- [5] K. M. Guckian, B. A. Schweitzer, R. X.-F. Ren, C. J. Sheils, D. C. Tahmassebi, E. T. Kool, *J. Am. Chem. Soc.* **2000**, *122*, 2213–2222.  
 [6] R. L. Letsinger, G. Zhang, D. K. Sun, T. Ikeuchi, P. S. Sarin, *Proc. Natl. Acad. Sci. USA* **1989**, *86*, 6553–6556.  
 [7] S. M. Gryaznov, D. H. Loyd, *Nucleic Acids Res.* **1993**, *21*, 5909–5915.  
 [8] C. F. Bleczynski, C. Richert, *J. Am. Chem. Soc.* **1999**, *121*, 10889–10894.  
 [9] All of the  $\alpha$ PNAs reported here possess the backbone shown in Scheme 1 and are described by the N-cap followed by the nucleobase sequence (N to C terminus from left to right). Electrospray ionization mass spectral (ESI<sup>+</sup>-MS) characterization data for N-capped  $\alpha$ PNAs:  $m/z$ : 4-phenylbutyryl-CTCCT: calcd 2811.41, found  $2812.61 \pm 0.41$ ; 4-(*p*-methoxyphenyl)butyryl-CTCCT: calcd 2841.42, found  $2842.36 \pm 0.13$ ; 4-(*p*-nitrophenyl)butyryl-CTCCT: calcd 2856.40, found  $2857.55 \pm 0.24$ ; 4-(2-naphthyl)butyryl-CTCCT: calcd 2861.43, found  $2862.68 \pm 0.40$ ; 4-(1-pyrenyl)butyryl-CTCCT: calcd 2935.44, found  $2937.02 \pm 0.39$ ; N-butyryl-CTCCT: calcd 2735.38, found  $2736.52 \pm 0.54$ ; N-hexanoyl-CTCCT: calcd 2763.41, found  $2766.01 \pm 1.19$ ; 3-cyclopentylpropionyl-CTCCT: calcd 2789.43, found  $2792.10 \pm 1.01$ ; 4-cyclohexylbutyryl-CTCCT: calcd 2817.46, found  $2818.41 \pm 0.74$ ; 4-cyclohexylbutyryl-CTCCT: calcd 2802.46, found  $2803.12 \pm 0.39$ ; 4-cyclohexylbutyryl-CCCCC: calcd 2787.46, found  $2787.83 \pm 0.06$ ; cheryl-CTCCT: calcd 3055.61, found  $3055.69 \pm 1.67$ .  
 [10] Thermal UV denaturation curves were obtained with sample solutions made by combining the N-capped  $\alpha$ PNA and ssDNA components (5  $\mu\text{M}$  each) in TE buffer (10 mM Tris-HCl, 1 mM EDTA, pH 7). These solutions were then incubated overnight at 4  $^\circ\text{C}$ . All measurements were conducted in a quartz cell (1 cm pathlength) equipped with a temperature probe. The absorbance at 260 nm was recorded as a function of temperature by using a Perkin–Elmer Lambda 20 UV/Vis spectrophotometer equipped with a PTP-1 Peltier System thermocontroller with heating/cooling rates of 1  $^\circ\text{Cmin}^{-1}$ . Below 20  $^\circ\text{C}$ , dry  $\text{N}_2$  gas was passed through the spectrophotometer sample chamber to prevent moisture condensation. Data was collected and evaluated by using the TempLab software package (version 1.5, Perkin–Elmer Corp., Norwalk, CT, USA). The melting temperature  $T_m$  (defined as the temperature at which 50% of a complex is dissociated into its constituent components) was determined from the inflection point maximum of the first derivative of the melting curves and is the average of two separate runs.  
 [11] For a given DNA target,  $d(\text{A}_3\text{-NNNNN-A}_3)$  (N = purine nucleobase), the level of hysteresis (difference between heating and cooling transitions) appears to be inversely proportional to G·C content and, for the most part, independent of N-cap structure. Thus, for 4-(cyclohexyl)butyryl-CTCCT· $d(\text{A}_3\text{-GAGGA-A}_3)$ ,  $\Delta T_m$  (heating–cooling) is about 3  $^\circ\text{C}$ , whereas no hysteresis is observed for 4-(cyclohexyl)butyryl-CCCCC· $d(\text{A}_3\text{-GGGGG-A}_3)$ . The only exception is the pyrene-containing N-cap, which shows no hysteresis and may be accelerating binding kinetics through a favorable intermolecular  $\pi$ – $\pi$  interaction prior to structural reorganization to give the final base-paired  $\alpha$ PNA·DNA complex.  
 [12] F. Cozzi, M. Cinquini, R. Annuziata, J. S. Siegel, *J. Am. Chem. Soc.* **1993**, *115*, 5330–5331.  
 [13] The N-cap hydrophobicity ( $\log P$  values) was calculated according to: A. Leo, C. Hansch, D. Elkins, *Chem. Rev.* **1971**, *71*, 525–616 (see Supporting Information).  
 [14] For a succinct introduction to the hydrophobic effect and its biological implications, see: A. Fersht, *Structure and Mechanism in Protein Science*, Freeman, New York, **1999**, chap. 11.

Received: June 6, 2000

Revised version: August 23, 2000 [Z 113]